KU LEUVEN

Proceedings of the
THIRD INTERNATIONAL

SLAG VALORISATION SYMPOSIUM

THE TRANSITION TO SUSTAINABLE MATERIALS MANAGEMENT

19-20 March 2013
Leuven, Belgium

Editors Annelies Malfliet, Peter Tom Jones, Koen Binnemans, Özlem Cizer, Jan Fransaer, Pengcheng Yan, Yiannis Pontikes, Muxing Guo, Bart Blanpain

THE IMPORTANCE OF MATERIALS PROPERTIES IN HIGH-TEMPERATURE PROCESSES

Kenneth C. MILLS[1], Muxing GUO[2]

[1] Department of Materials, Imperial College, London SW& 2AZ, UK
[2] Department of Metallurgy and Materials Engineering, KU Leuven, 3001 Heverlee, Belgium

kcmills@talktalk.net, muxing.guo@mtm.kuleuven.be

Abstract

In high temperature processes, physico-chemical properties of the phases involved have proved useful in identifying the mechanisms responsible for process problems and product defects. However, recently mathematical models have developed to the stage where they can now be used to identify these mechanisms. These models require reliable values for the thermo-physical properties for the various phases involved in the process. The thermo-physical properties of slags are very dependent upon slag structure. The factors affecting slag structure are outlined and the ways in which structural factors affect various physical properties are described. Finally, the manner in which the following properties (liquidus temperature; viscosity, surface and interfacial tension; thermal conductivity and enthalpy) can be manipulated to optimise process control and product quality is demonstrated for various industrial processes. The same techniques can be used for valorisation activities.

Introduction

Physico-chemical property measurements for materials involved in many high-temperature processes have proved useful in identifying the cause of problems with process control and product quality. These materials involve metals, slags and refractories. The unofficial First and Second Laws of High Temperatures state, respectively, *"At high temperatures everything reacts with everything else"* and "*They react very quickly and the situation worsens quickly as the temperature increases"*. Consequently, problems with process control and product quality are frequent in high-temperature processes. Property data have proved very useful in the past in solving these problems. A classical example of this is *variable weld penetration* in Tungsten Inert Gas (TIG) welding [1-3]. This technique is frequently used as a robotic process to make thousands of repetitive welds; the optimum welding conditions to obtain deep welds (Figure 1b) are established in preliminary studies. However, it has been found that when these conditions are applied to another batch of steel (fully meeting the materials specification) they produced poor weld penetration (Figure 1a). This problem is known as *variable weld penetration*.

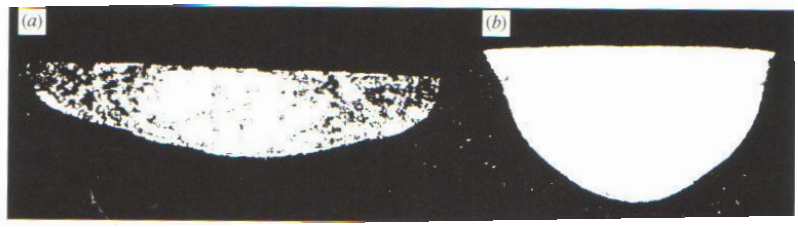

Figure 1: Photographs showing variable weld penetration and (a) poor weld penetration and (b) good weld penetration

There are several forces operating in the weld pool, namely, Buoyancy forces, Lorenz (electro-magnetic) forces and aerodynamic drag forces (caused by the flow of inert gas over the liquid metal surface) plus Marangoni (or thermo-capillary) forces (Figure 2)[1-3]. The latter arise from surface tension gradients resulting from steep temperature gradients; the temperatures at the centre and the edge of a weld pool are ca. 2500 and 1500^{o}C, respectively, thus gradients of 500^{o}C mm^{-1} are normal. Marangoni flows always occur from low surface tension to high surface tension.

Surface tension measurements (Figure 3) were carried out on more than 50 steels with known "poor" or "deep" weld penetration[2,3]. Poor weld penetration correlated with negative values of dγ/dT, high values of γ and S contents of <30 ppm. Deep weld penetration correlated with positive gradients (dγ/dT), lower values of γ and S contents >60 ppm.

Consequently, it was proposed that Marangoni forces were dominant in the weld pool and that variable weld penetration was caused by surface tension gradients arising from the temperature gradients on the surface of the weld pool [1].

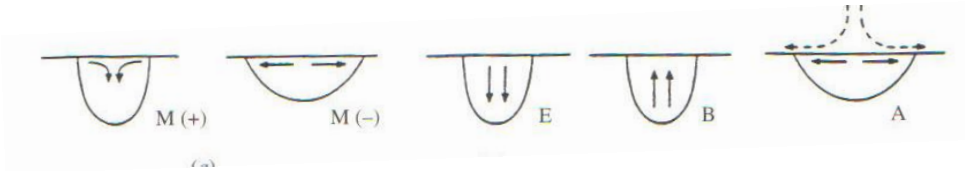

(a) (b) (c) (d)

Figure 2: Schematic diagram showing the fluid flows resulting from different mechanisms acting in the weld pool (a) Marangoni forces (+) = (dγ/dT =positive); Marangoni forces (-) = (dγ/dT =negative) (b) E= Lorenz electro-magnetic forces (c) B= Buoyancy forces (d) A= aerodynamic drag forces

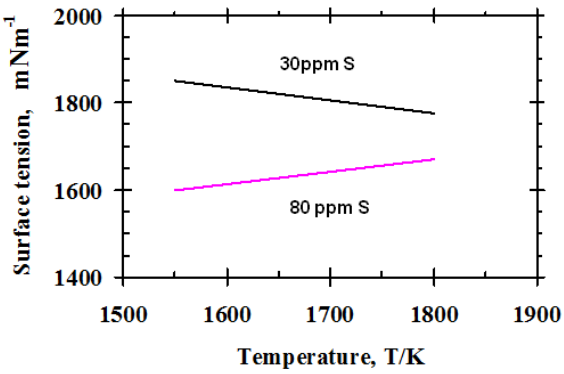

Figure 3: Surface tension (γ) and (dγ/dT) of steels with 30 and 80 ppm S as a function of temperature[2,3]

For low S steels the surface flow is radially outward and takes hot metal from the centre to the edge of the weld pool where melt-back results in a wide, shallow weld (Figure 4a) [1-3]. In contrast, for high S steels the Marangoni flow results in a radially-inward and then downward flow of hot metal in the centre of the weld (Figure 4b) so that melt-back occurs at the bottom of the pool creating a deep weld (Figure 4b)[1-3]. Thus measurements of surface tension were able to show that variable weld penetration resulted from differences in surface tension gradients in the weld pool which, in turn, arose from minor (ppm level) differences in the sulphur content of the steel.

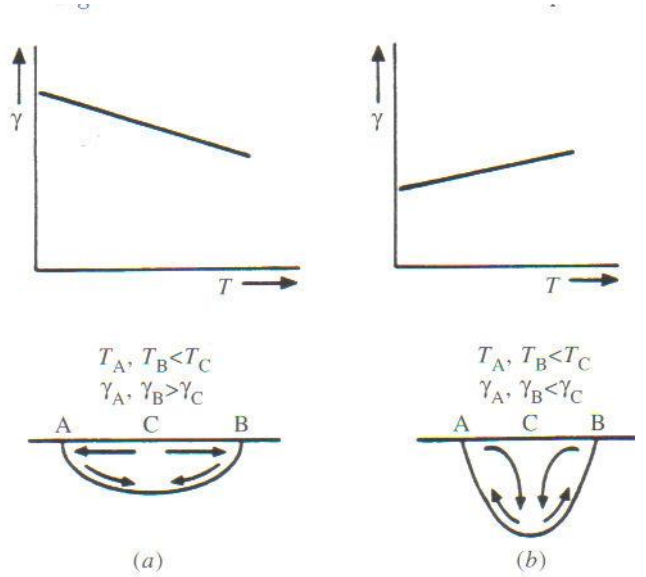

Figure 4: Schematic diagrams showing how fluid flows in weld pool for (a) low S (<50 ppm) steel and (b) high S (>50 ppm) steel are affected by surface tension gradients (dγ/dT) [1-3]

However, in the past decade a new demand for property data has arisen, namely, as input data in mathematical models of processes. In recent years mathematical modelling has proved to be a valuable tool in minimising process problems. However, these models require accurate values for the properties of the materials involved. One problem continually encountered in high-temperature processes is that you can not see into the vessel/mould. Consequently, we must rely on data from sensors to deduce the mechanisms underlying the problem. However, mathematical models have now developed to the state where they can provide us with insights into the mechanisms involved in high temperature processes; examples of model predictions are shown below in Figure 10.

If you were designing a new process you would use various mathematical models to check the viability of the process, namely:

(i) A thermodynamic model to determine the viability of the process and the optimum conditions.
(ii) A kinetic model to show productivity will be high enough.
(iii) A fluid flow and heat transfer model to anticipate process and product-quality problems.
(iv) Economic and Environmental models to study the financial and environmental impact of the process.

In this paper the principal focus will be on (iii) above, *i.e.* the properties involved in fluid flow and heat transfer and case histories are given below to illustrate the importance of slag properties in optimising process control and product quality. The principal focus is on the optimisation of the process including slag processing for valorisation.

Properties of slags

Many high-temperature processes involve metal, slag and refractory phases. In this study our main focus will be on the properties of the slag phases.

Structure of slags

It should be noted that slags are ionic and slag-metal reactions such as Equation 1 are better expressed in the form of Equation 2 where the underline denotes dissolved in the metal.

$$4\underline{Al}_{steel} + 3SiO_{2slag} \rightleftharpoons 3\underline{Si}_{steel} + 2Al_2O_{3slag} \quad (1)$$

$$4\underline{Al} + 3Si^{4+} \rightleftharpoons 3\underline{Si} + 4Al^{3+} \quad (2)$$

Role of the slag phase

Slags play a vital role in many pyro-metallurgical processes, they carry out in the following functions:

(i) They seal off the metal phase from the atmosphere and prevent oxidation of the metal.
(ii) They provide thermal insulation which prevents the metal from freezing.
(iii) Slag/metal reactions remove deleterious elements (eg. S) from the metal
(iv) They aid the removal of non-metallic inclusions from the metal.

Slag structure

The properties of silicate slags and glasses are very dependent upon the structure. The basic building block in silicates is a Si^{4+} ion surrounded by 4 O^{2-} ions in a tetrahedral array (Figure 5). Each of these O^{2-} ions allows one Si^{4+} tetrahedron to link to another tetrahedron. Thus in pure SiO_2 the structure consists of Si^{4+} tetrahedra joined via O^{2-} ions at the corners to other tetrahedra in a 3-dimensional array; these O^{2-} ions are known as *bridging oxygens (BO).* Thus Si is said to exhibit 4-fold coordination and the bonding is covalent [4].

When cations such as Na^+ or Ca^{2+} are added they tend to break the network and form O^--Na^+ bonds (Figure 5) or O^--Ca^{2+}-O^- bonds, respectively ; thus the cations are referred to as *network-breakers* and the bond formed as *Non-Bridging Oxygens (NBO)*. These cations (*e.g.* Na^+ or Ca^{2+}) are arranged in octahedral geometry and exhibit, in general, 6-fold coordination [4].

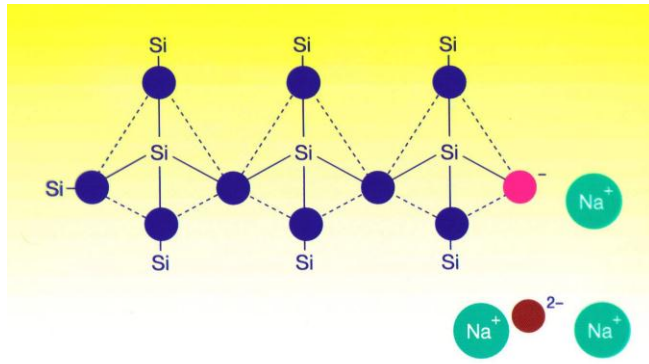

Figure 5: Schematic drawings showing (a) Si^{4+} tetrahedron and joining of tetrahedral through O^{2-} ions and at bottom free O's formed in de-polymerised melts (ca. Q<1 where Q is defined in Equation 4)

When Al_2O_3 is added to a silicate slag the Al^{3+} ions are incorporated into the Si^{4+} network but the Al^{3+} needs a cation (Na^+ or half of Ca^{2+}) in close proximity for charge-balancing *i.e.* to form $(NaAl)^{4+}$ (Figure 6) [4]. Cations on charge-balancing duties are not available for network-breaking. Thus Al^{3+} tends to show 4-fold coordination (denoted $^{(4)}Al$). With large additions of Al_2O_3 there is the possibility of $^{(5)}Al$ and $^{(6)}Al$ formation[5,7].

The parameter NBO/T is often used to represent the *degree of de-polymerisation* of the melt (Equation 3)

$$NBO/T=2\ (\Sigma X_{MO} + \Sigma X_{M2O} - X_{Al2O3})/\ (X_{SiO2} + 2\ X_{Al2O3}) \qquad (3)$$

where X is the mole fraction and $X_{MO} = X_{MgO} + X_{CaO} + X_{BaO} + X_{FeO} + X_{MnO} + ...$ and $X_{M2O} = X_{Li2O} + X_{Na2O} + X_{K2O}$.

We prefer to use the parameter, Q (Equation 4) which is a measure of the *degree of polymerisation* and which is calculated via Equation 4.

$$Q= 4-(NBO/T\ ) \qquad (4)$$

It might be expected that TiO_2 would behave like SiO_2 and would be incorporated into the silicate network but the $CaO\text{-}SiO_2\text{-}TiO_2$ system exhibits a large miscibility gap; although there are some Si-O-Ti bonds formed there is a preference for Ti-O-Ti and Si-O-Si bond formation which affects both the structure and the properties. It might also be expected that Cr_2O_3 and Fe_2O_3 would behave like Al_2O_3. This is largely true for Cr_2O_3 but Fe_2O_3 acts partially as a network former and partially as a network-breaker.

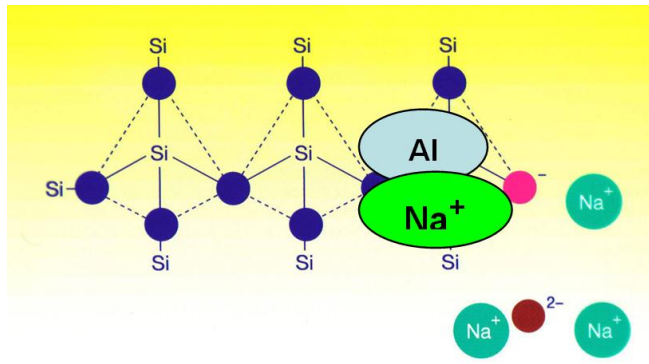

Figure 6: Schematic diagram showing incorporation of Al^{3+} into Si^{4+} network and showing charge-balancing cations

Some silicates exist in both crystalline and glassy forms. In crystals the atoms or ions are in fixed positions whereas there is much more disorder in the rapidly-quenched glassy phase. Thus the entropy of the glassy phase is higher than that of the crystal ($S_{gl}>S_{cryst}$) and the additional entropy in the glass (arising from the disorder) is referred to as *configurational entropy*.

When a glass or crystal is heated the disorder tends to increase. At lower temperatures the thermal vibrations are insufficient to cause much disorder in the quenched glass but when the glass reaches the glass transition temperature (T_g) there is a rapid increase in disorder as the glass is transformed into a supercooled liquid (*scl*). This increase in configurational entropy (ΔS_{Tg}^{config}) is accompanied by a *step-increase* in heat capacity and 3-fold increase in thermal expansion coefficient (α).This transition does not occur for crystals so C_p and S values for the crystal phase are lower than those for the *scl*. However at higher temperatures crystals exhibit an entropy of fusion (ΔS^{fus}) at T_{liq} which is absent for the *scl*.

The nature of the cations can also affect the structure and the properties of silicate slags[7] but their effect is much smaller than the degree of polymerisation. Cations can affect the structure of the melt, *e.g.* reaction 5 is promoted by cations with high field strength (*ie.* high values of z/r^2) which, in turn, affects the properties.

$$2Q^n = Q^{n-1} + Q^{n+1} \quad (5)$$

Alternatively, some properties are affected by the size of the cations (*ie*. by their radius = r).

Effect of structure on properties

<u>Viscosity (η), electrical resistivity (R), conductivity (κ) and diffusion coefficient (D)</u>

Viscosity (η) is a measure of the resistance to the movement of one layer of molecules over another layer of molecules. The viscosity increases with increasing degree of polymerisation (Q, Figure 7a) and decreasing temperature, which is usually represented by the Arrhenius relation shown in Equation 6:

$$\eta = A_A \exp(B_A/T) \quad (6)$$

where η is in dPas, T is in K, A_A is the pre-exponential term and B_A represents the activation energy (E) term (B = E/R* where R* is the universal Gas constant. The temperature dependence in the *scl* phase is much stronger and is represented by the Vogel-Fulcher- Tamman relation.

$$\eta = A_V \exp(B_V/(T-T^o)) \quad (7)$$

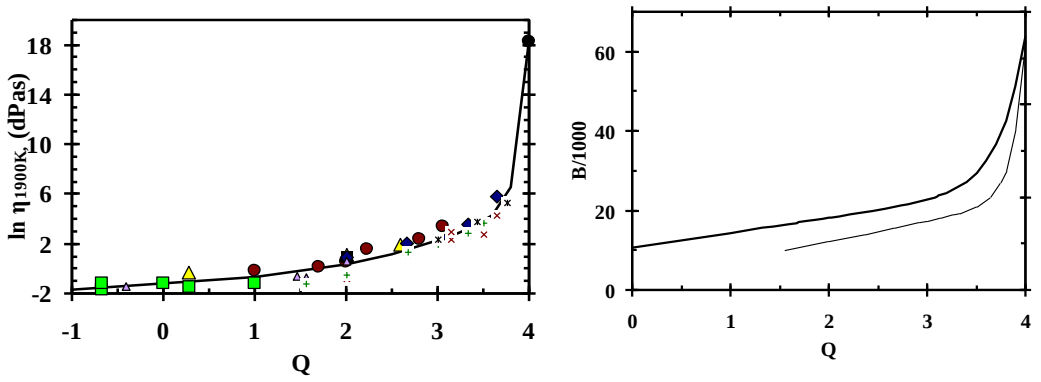

(a) **(b)**

Figure 7: (a) Viscosity (ln η_{1900K}) and (b) activation energy parameter, B_η, for MO-SiO_2 and M_2O-SiO_2 systems for viscosity (upper curve = MO; lower curve = M_2O) [8]

It can be seen from Figure 7 that both the viscosity and the activation energy term, B, are sensitive functions of the degree of polymerisation, Q.

The electrical conductivity (κ) represents the ability of the ions to move under an applied electrical field; the cations are the mobile species since the anions (silicate ions) are too large and sluggish. The electrical resistivity (R = 1/κ) is the resistance to the cation movement and is therefore the equivalent of viscosity. There are two factors affecting the resistivity, namely, (i) the resistance to the movement of cations

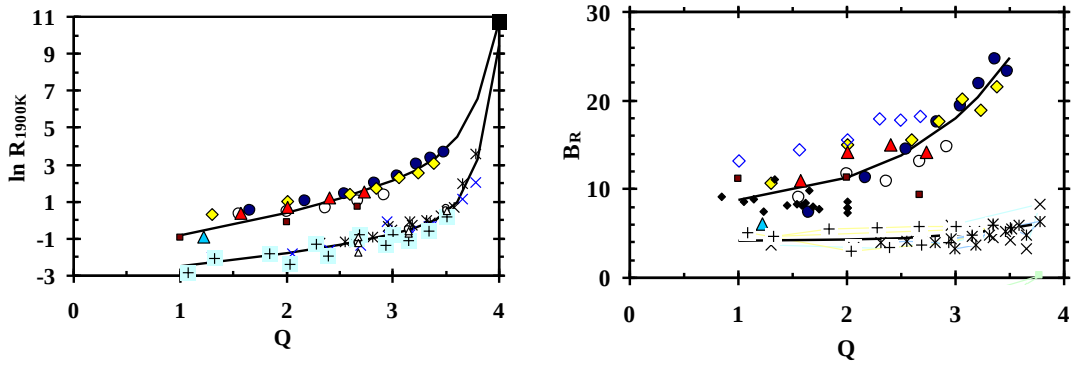

Figure 8: (a) Electrical resistivity (ln R_{1900K}) and (b) activation energy term, B_R, of MO-SiO_2 and M_2O-SiO_2 systems as a function of the parameter Q (upper curve = MO and lower curve = M_2O); + = LS; x = NS; * = KS; o = CS; ▲ = MS; ◊ = SrS; ● = BS; ▲ = FS; ■ = MnS; ♦ = MFS where B = BaO; C = CaO; F = FeO; K = K_2O; L = Li_2O; M = MgO; Mn = MnO; Sr = SrO; N = Na_2O and S = SiO_2 [8]

and (ii) the number (n) and mobility of the cations; note Na_2O produces 2 cations whereas CaO only produces 1 which accounts for the differences between the curves for M_2O and MO in Figure 8a and 8b.

The factors affecting the diffusion coefficient (D) are very similar to those for the electrical conductivity and thus a plot of (1/D) versus Q looks very similar to Figure 8.

Density (ρ) and thermal expansion (α, β)

Thermal expansion in slags results from the asymmetry of the thermal vibrations produced when a slag is heated. The thermal expansion coefficient (α) decreases with increasing polymerisation (Q) and decreasing field strength (*i.e.* z/r^2)[7]. However, for glassy samples there is a large increase in α at the glass transition temperature and $\rho_{crys} > \rho_{scl}$ for temperatures between T_g and T_{liq}; however, this is compensated by a change in density for the crystalline phase at T_{liq} which is absent for the *scl* phase.

The density of the crystalline phase is slightly higher than that of the glass because of the better packing in the crystal phase.

Surface and interfacial tension (γsl, γmsl)

Surface tension (γ) is a *surface property* and not a *bulk property*. Certain constituents with low surface tension (known as *surfactants*) tend to inhabit the surface layer of the melt and cause both a marked decrease in surface tension (γ) and cause (dγ/dT) to become progressively more positive. Typical surfactants in metals are *soluble* sulphur and oxygen (*i.e.* not sulphides and oxides); *e.g.* 50 ppm S in Fe causes a decrease in γ_m of 25%. The surfactants in slags do not have as dramatic effect as S and O in Fe but do influence the slag surface tension; typical surfactants in slags are the fluxes used in most slags, B_2O_3, CaF_2, K_2O and Na_2O.

The interfacial tension between metal and slag (γ_{msl}) is given by Equation 8 where ϕ is an interaction coefficient[9]:

$$\gamma_{msl} = \gamma_m + \gamma_{sl} - 2\phi(\gamma_m \gamma_{sl})^{0.5} \quad (8)$$

The principal factor affecting γ_{msl} is γ_m since for most metals $\gamma_m \approx 4\ \gamma_{sl}$ and thus γ_{msl} is greatly dependent upon the *soluble* S and O contents of the metals.

Thermal conductivity (k) and diffusivity (a)

Heat transfer across a slag layer at high temperatures is an exceedingly complex process since it involves several different heat transfer mechanisms, namely, *thermal conduction*, *radiation* and for melts, *convection*. In semi-transparent media, like glasses and slags, the measured (or effective) thermal conductivity (k_{eff}) (Equation 9)

contains contributions from both the lattice conductivity (k_{lat}) and the radiation conductivity (k_R) which involves absorption and re-emission of IR radiation by each successive layer in the sample. Values of k_R were found to increase with increasing sample thickness (d) until it reaches a critical point; the sample is denoted as *optically-thick* at this critical point which occurs when $\alpha^*d > 3$ where α^* is the absorption coefficient) and thereupon k_{eff} remains constant[10]. Values of k_R can be calculated for optically-thick conditions using Equation 10 and the dependence on T_K^3 ensures that k_R increases dramatically at high temperatures.

$$k_{eff} = k_{lat} + k_R \quad (9)$$

$$k_R = 16\,\sigma\, n^2\, T_K^3/3\,\alpha^* \quad (10)$$

where σ = Stefan-Boltzmann constant and n = refractive index. These k_R contributions can be reduced by (i) absorption of IR radiation by FeO, NiO *etc* in the slag and (ii) scattering of IR radiation by crystals.

The lattice conductivity (k_{lat}) is affected by several factors:

(i) whether the sample is crystalline or glassy since kcrys ≈ 2kgl due to the closer packing of atoms in the crystal (*cf.* glass) and which results in higher conductivity values.
(ii) Porosity in the sample, with klat decreasing with increasing porosity.

There is a paradox associated with the heat transfer in a slag layer at high temperatures, namely, that crystallites in the slag reduce the heat flux (q) despite the fact that $k_{crys} \approx 2k_{gl}$; this is due to the much larger reduction in the k_R due to the scattering of the IR radiation by the crystals.

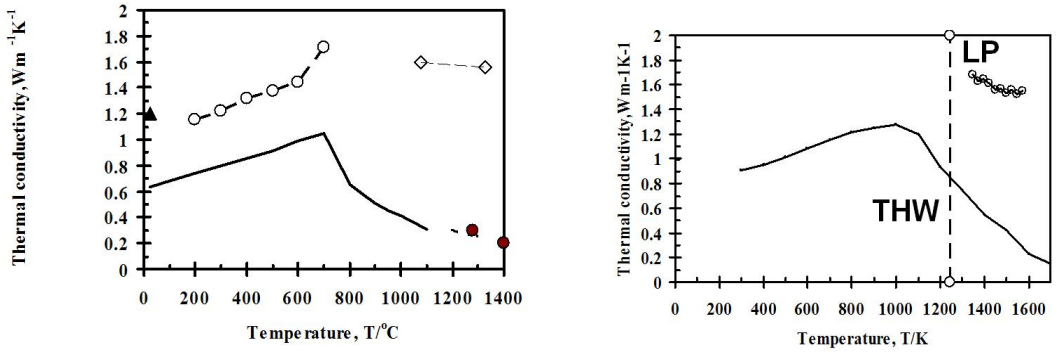

Figure 9: Thermal conductivity as a function of temperature for (a) Mould fluxes; line, ● = k_{THW} results and ◊,o= k_{LP} results and (b) Na_2O-CaO-SiO_2 slags of similar composition using the laser pulse (LP) and transient hot wire (THW) methods

One further complication has been identified recently. It has been found that the thermal conductivity values for slags of almost identical composition are very different when measured using the two most popular techniques (*i.e.* laser pulse (LP) and transient hot wire (THW)). It can be seen from Figure 9 that (i) the k-T relations for k_{THW} and k_{LP} are very different and (ii) for the liquid, $k_{LP} \approx 7\ k_{THW.}$ These differences have been ascribed to (i) k_R contributions in the LP method and (ii) electrical leakage in THW measurements, but at the present time the problem is unresolved.

Manipulation of slag properties for process optimisation

In this section we show how slag properties can be manipulated to optimise process control and product quality. The same techniques could be used in valorisation activities.

Manipulation of melting characteristics

There are cases where the combined attack of slag and metal on the refractory has proved so severe that otherwise-viable processes have had to be abandoned. One method used to extend refractory life is to distribute the molten slag around the slag walls to create a "*freeze lining*" of slag in a water-cooled vessel; this sacrificial lining then protects the refractory from further attack. Freeze linings are used in various processes *e.g.* the Lurgi coal combustion and Basic Oxygen Steelmaking (BOS) processes. In the LD version of the BOS process, the carbon is removed from the molten mixture of pig iron (from the blast furnace) and scrap by blowing oxygen at supersonic speeds. A slag phase is formed by SiO_2 (from oxidation of Si in the pig-iron), FeO and added CaO. Wear of the refractories is significant because of the great turbulence of the gas, slag and metal phases. Thus there is considerable *"downtime"* in the process to replace refractories. "*Slag splashing"* was developed in the USA and China to extend refractory life and minimise *"downtime"*. In this process when the metal has been drained from the vessel, the lance is lowered and the slag is splashed around the walls using a gas jet, thereby creating a freeze lining. Several companies tried slag splashing but found the benefits were outweighed by a rapid loss of the freeze lining and contamination of the metal. Some companies persisted and optimised the conditions for slag formation. *Ad-hoc* research showed that optimum conditions required that slag contains ca 13% FeO and >8% MgO. It was subsequently shown that these levels of FeO and MgO avoided formation of low-melting ferrites and ensured that high-melting $MgOFe_2O_3$ was formed[11]. Refractory lives of >50000 heats have been recorded with slag splashing. Thus manipulation of the slag composition to provide high-melting phases resulted in significant valorisation for the BOS process.

Manipulation of the slag viscosity

In high-temperature processes such as Coal Gasification or in smelting operations it is important to drain the slag from the vessel. The drainage rate is inversely related to the slag viscosity and viscosities of ca 1 Pas are needed to achieve reasonable drainage times. In the case of coal gasification the mineral matter (or ash) forms a highly-viscous slag (with Q > 3). We have seen above (Figure 7) that viscosity is primarily affected by the degree of polymerisation. Q, and it is necessary to reduce Q to obtain the required viscosity. CaO additions reduce both Q (and hence the viscosity) and the T_{liq} for the slag. The low melting regions of the $CaO\text{-}SiO_2$ and $CaO\text{-}Al_2O_3$ systems lie in a narrow compositional range X_{CaO} = (0.4-0.5) and (0.5-0.7) respectively. Thus the CaO additions should be carefully adjusted to ensure they fall within these limits since the presence of any solid particles significantly increases the viscosity.

Disasters (where the slag solidifies in the vessel) have occurred when a fixed amount of CaO has been added to the slag, for instance, when the normal coal has been replaced by a low-ash coal; since the latter creates a much lower slag volume, the fixed CaO addition results in the formation of a high- melting, CaO-rich slag.

It should be noted that when the slag is drained from a vessel it leaves a thin layer of slag on the vessel wall ("*ladle glaze*") this slag can become a source of slag inclusions in the next heat [12]; where un-contaminated metal is required it is necessary to "*wash*" the vessel to minimise the contamination.

Surface and Interfacial tension

Entrainment of slag and metal

The entrapment of metal droplets in the slag and slag droplets in the metal are serious problems in metal processing since:

(i) in the production of precious metals and copper *etc* metal droplets trapped in the slag represent a significant loss of valuable metal.
(ii) in the continuous casting of steel entrapped slag causes significant deterioration in the mechanical properties of the steel.

Metal entrapment and slag entrapment are caused by the differences in velocities of the metal and slag phases and tend to be accentuated by high velocities in the two phases. Take for instance, the continuous casting of steel, high production rates involve using high flow rates of molten steel in the nozzle (SEN) and more importantly, in the mould. These high flow rates give rise to turbulent metal flows in the mould resulting in both the formation of standing waves (Figure 10a) and vortices at the metal/slag interface (Figure 10b)[13].

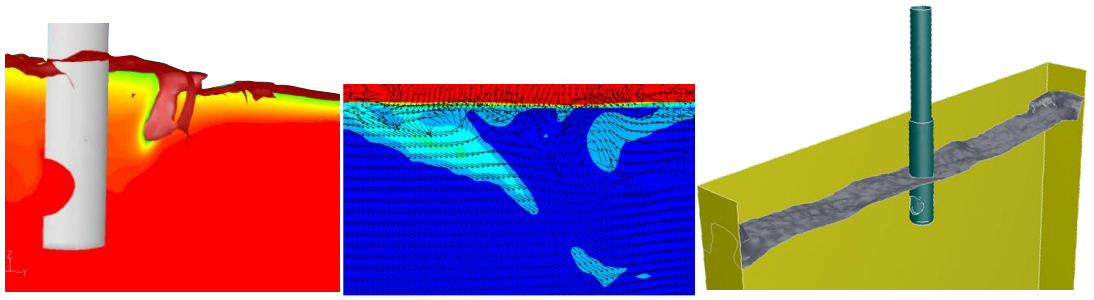

(a) (b) (c)

Figure 10: Mathematical model predictions for the formation of (a) standing wave (b) Karmen vortex near the nozzle and (c) *necking* and *detachment* of slag in metal [13]

The flow patterns in the mould are shown in Figure 11a. The radially-inward flow of metal is much higher than that of the slag since the viscosity of the slag is *ca.* 50 times higher than that of the slag. These differences in the flow velocities result in "*necking*" of the slag filament and eventually "*detachment*" and "*capture*" of the slag droplet (Figure 11b, steps 3 and 4 respectively). This mechanism was identified by water-modelling studies[14,15]. However, recently a mathematical model has been proposed[13] which incorporates the fluid flow (metal and slag), heat transfer and solidification of the steel; this model satisfactorily predicts the formation of standing waves, vortices and slag necking and detachment (Figure 10).[13]

Tsutsumi *et al.*[15] performed water modelling studies and found that the mass of entrapped slag (m_{entrap}) caused by Karman vortices (Equation 11) was affected by both slag viscosity (η_{sl} in Pas) and interfacial tension (γ_{msl}). Increased interfacial tension can best be achieved by lowering the S and O contents of the metal but decreasing the B_2O_3, K_2O and CaF_2 in the slag would also help in reducing entrapment.

$$m_{entrap}=1.06x10^{-7} (\eta_{sl})^{-0.255}. (\gamma_{msl})^{-2.18} \quad (11)$$

It would seem probable that similar mechanisms would be responsible for metal entrapment in the slag (*e.g.* from vortex and standing wave formation) especially where rotary furnaces are involved. The mass of entrapped slag can be reduced by increasing the interfacial tension. However, the time taken for the metal droplets to sink back into the metal phase would be increased with increasing slag viscosity.

<u>Other processes affected by surface and interfacial tension</u>

Surface and interfacial tensions are involved in a number of pyro-metallurgical processes *e.g.*:

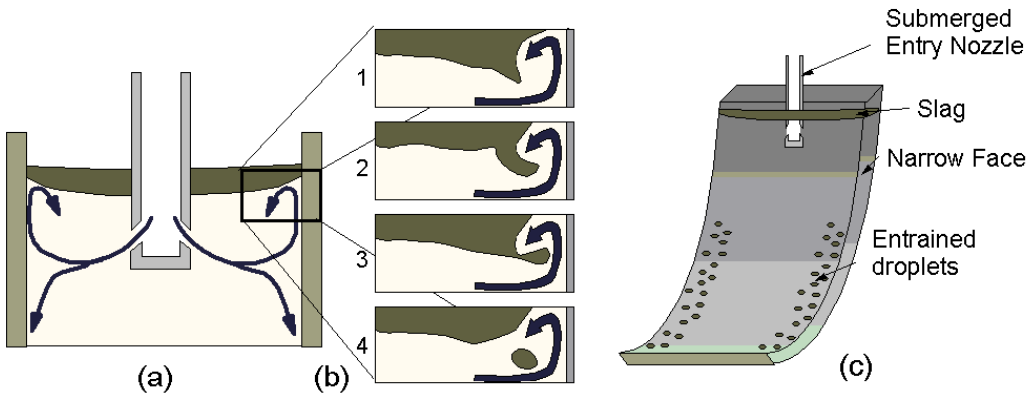

Figure 11: Schematic diagrams showing (a) the fluid flow in the metal in the continuous casting mould (b) the mechanism responsible for necking and detachment and (c) the location of slag inclusions on the steel slab

(i) the removal of inclusions from the metal by attachment to bubbles.

(ii) the formation of scales on the surface of continuously-cast slabs where fluxes rich in Na_2O, K_2O and Li_2O tend to adhere strongly to the steel furnace and do not fall off in the spray chambers; the SiO_2 in these fluxes reacts with FeO (formed by oxidation of the steel surface) to form $FeSiO_3$ which forms the scale.

(iii) the separation of droplets of Fe, Cu and precious metals from the slag for the recovery of these metals in slag valorisation processes.

Manipulation of heat transfer through a slag "freeze lining"

It was pointed out above (in the section on thermal conductivity) that heat transfer process in a slag layer at high temperatures is exceedingly complex. The primary purpose of a freeze lining is to protect the refractory but it also provides valuable thermal insulation. In the continuous casting of steel, liquid slag penetrates between the shell and the mould (Figure 12) and solidifies to form a "*slag film*" (*ie.* a freeze lining) which consists of a solid layer (*ca*. 2 mm thick) and a liquid layer (0.1 mm thick). The thickness of the solid layer (d_s) determines the heat transfer and the thickness of the liquid layer (d_l) the level of lubrication[13]. Medium–carbon (MC) steels are prone to *longitudinal cracking* and the remedy is to ensure the steel shell is both thin and uniform. This is achieved by (i) minimising (d_s/k_{eff}) and (ii) reducing radiation conductivity (k_R) by designing a slag film which develops a high crystalline fraction to scatter the radiated heat. This is achieved by selecting the slag film to have a high T_{liq} (to give a thick d_s) and a high basicity (*i.e*. $\%CaO/\%SiO_2$) to ensure there is significant crystallisation. In contrast, high-carbon (HC) steels are prone to *"sticker breakouts"* where steel escapes from the mould because the HC shells are weak. The solution is

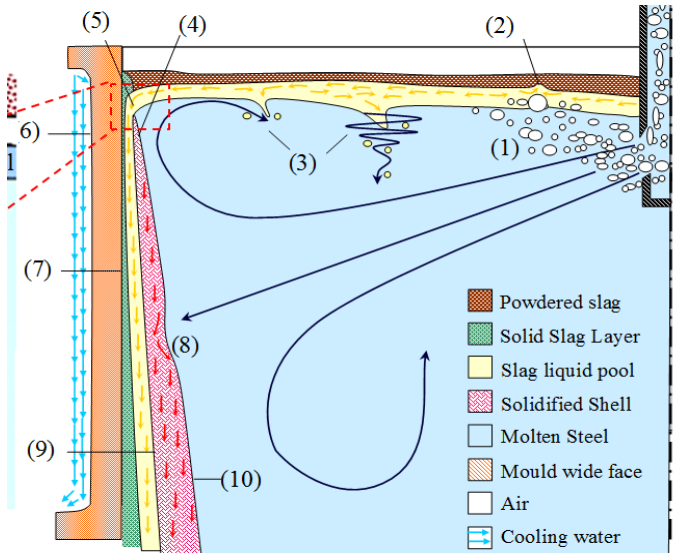

Figure 12: Schematic diagram showing half-section of continuous casting mould; steel shell = 4 & 10; liquid slag film = 9; solid slag film = 7; mould = 6 [13]

to create a thick shell (*i.e.* the opposite of that for MC steels) and this is achieved by using a slag with (i) a low T_{liq} (to minimise d_s) and (ii) a low basicity to promote high heat fluxes *via*.k_R. Thus the composition can be manipulated to obtain the required level of heat transfer.

Enthalpy of slag at high temperatures

Energy costs constitute about 30% of the total costs in steelmaking. Although several improvements to energy efficiency have been made in recent years, the energy costs remain high. One source of heat wastage is the heat tied up in molten slag phase which is just poured off. A few years ago, Mr. R. Tata, the chairman of Tata Steel was visiting the BOS plant in the steelworks at Jamshedpur and noticed a flame emanating from the slag pit where molten slag was being cooled (and granulated) with water. He enquired about the cause of the flame and was told it was hydrogen burning; the hydrogen being formed by the decomposition of the cooling water. He then suggested that they should try to harvest the hydrogen and a research programme was initiated. The major problem in hydrogen harvesting lies in the separation of oxygen (from the decomposition and the atmosphere) from the hydrogen. Tata Steel has successfully produced a gas containing >70% hydrogen with the remaining gas consisting of nitrogen and CO_2.The proof of concept was then demonstrated using a pilot LD plant and is now being applied in a plant used for the production of ferro-alloys. It has been calculated that if this technology is successful, the savings in energy for a steelworks producing 6 million tonne of steel *p.a*. would be 30 million dollars *p.a*. The hydrogen formed can be used either to produce clean energy or for the direct reduction of iron ore; it will be used initially as a heat source in the ferro-alloy plant.

Discussion

We have seen above that property measurements can be exceedingly useful in identifying the causes of process problems. We have also noted that property values are needed for input data into mathematical models and this requirement is becoming ever-more important. Furthermore, mathematical models have proved to be capable of identifying the causes of process problems and product defects and these models will be used to optimise the process and may also prove useful in valorisation operations.

However, there is a wide-range of compositions used in high-temperature processes (*eg.* the continuous casting process outlined above) and it is unrealistic to make all the required measurements on such a wide range of materials. Consequently, there will be an increasing demand for models to calculate property values from chemical composition, which is available on a routine basis. There are some extant models available to calculate properties but, in general, the wider the range of slag composition covered, the worse the prediction. This is because the properties usually reflect the structure. The models which calculate properties for a wide compositional range try to describe the degree of polymerisation, using functions like Q (see Figures 7 and 8), (NBO/T) or thermodynamic functions; they then apply corrections for cation effects. However, certain oxides (*eg.* TiO_2) cause changes to the slag structure (such as changes in the coordination of Ti^{4+} cation or a preference for the company of other Ti^{4+} ions rather than Si^{4+} ions). Such structural features are not included in the present models and more detailed structural information may be needed to derive accurate thermo-physical properties of slags.

Conclusions

1. The thermo-physical properties are very dependent upon slag structure.
2. Mathematical models will be used to gain insights into process problems and product defects and this requires the need for reliable thermo-physical property values for slags.
3. Mathematical models will be developed to estimate the required property data from chemical composition; however, to obtain highly accurate property estimations it may be necessary to incorporate structural features (like changes in cation coordination) which are not covered at the present time
4. Knowledge of the factors affecting physical properties allows one to manipulate these properties in order to optimise these processes (including valorisation activities).

References

1. C.A. Heiple and J.R. Roper, “Mechanism for minor element effect on GTA fusion zone geometry”, *Welding Journal,* **61** 97s-102s (1982).
2. K.C. Mills, B.J. Keene, R.F. Brooks and A. Shirali, “Marangoni effects on welding”, *Phil. Trans. Royal Soc, London, **A*** **356** (1739) 911-925 (1998).
3. K.C. Mills and B.J. Keene, “The factors affecting variable weld penetration”, *Intl. Materials Reviews,* **35** 185-316 (1990).
4. B.O. Mysen, “Relationships between silicate melt structure and petrologic processes”, *Earth Science Reviews*, **27** (4) 281-365 (1990).
5. G.S. Henderson, “The structure of silicate melts: A glass perspective”, *The Canadian Mineralogist,* **43** (6) 1921-1958 (2005).
6. J.F. Stebbins, I. Farnan and X. Xue, “The structure and dynamics of silicate liquids: A view from NMR spectroscopy”, *Chemical Geology,* **96** (3-4) 371-385 (1992).
7. K.C. Mills, L. Yuan, Z. Li, G.H. Zhang and K.C. Chou, “A review of the factors affecting the thermophysical properties of silicates”, *High Temp. Materials & Processes*, **31** (4-5) 301-321 (2012).
8. K.C. Mills, L. Yuan, Z. Li and G.H. Zhang, “Estimating the electrical and thermal conductivities of slags”. In *Proceedings of 5th Intl. Cong. Of Science and Technology of Steelmaking,* Dresden, Germany, 2012, to be published in *High Temp.- High Pressure* (2013).
9. T. Tanaka, M. Nakamoto and J. Lee, “Evaluation of surface properties of liquid alloys and molten ionic mixtures for metal separation”, in *Proceedings of Metal Separation Technology*, 135-142, Edited by R.E. Aune and M. Kekkonen, publ. Helsinki Univ. Technol., Copper Mountain, USA, June 20-24, 2004.
10. R. Gardon, “A review of radiant heat transfer in glass”, *J Amer. Ceram. Soc*., **44** (7) 305-312 (1961).
11. K.C. Mills, Y. Su, A.B. Fox, Z. Li, R.P. Thackray and H.Tsai, “A review of slag splashing”, *ISIJ Intl.,* **45** (5) 619-633 (2005).
12. S. Riaz, K.C. Mills and K. Bain, “Experimental examination of slag/refractory interface”, *Ironmaking and Steelmaking,* **29** (2) 107-113 (2002).
13. K.C. Mills, P.E. Ramirez-Lopez and P.D. Lee, “Some insights into mechanisms involved in continuous casting”, *High Temp. Materials & Processes,* **31** (3) 221-229 (2012).
14. S. Feldbauer and A.W. Cramb, “Insights into slag entrainment in the mold of a continuous caster”, in *Proceedings of 13th PTD Conf.*, 327-342, Nashville, TN, USA, 1995.
15. K. Tsutsumi, K. Watanabe, M. Suzuki, M. Nakada and T. Shiomi, “Effect of properties of mold powder entrapped in molten steel in a continuous casting process”, in *Proceedings of VII Intl. Conf. on Molten slags, fluxes and salts,* 803-806. South African Institute of Mining and Metallurgy, Johannesburg, Republic of South Africa, 2004.